

# Assessment of an Advanced Monoenergetic Reconstruction Technique in Dual-Energy Computed Tomography of Head and Neck Cancer

Moritz H. Albrecht · Jan-Erik Scholtz · Johannes Kraft ·  
Ralf W. Bauer · Moritz Kaup · Patricia Dewes · Andreas M. Bucher ·  
Iris Burck · Jens Wagenblast · Thomas Lehnert · J. Matthias Kerl ·  
Thomas J. Vogl · Julian L. Wichmann

Received: 1 September 2014 / Revised: 5 December 2014 / Accepted: 21 January 2015  
© European Society of Radiology 2015

## Abstract

**Objectives** To define optimal keV settings for advanced monoenergetic (Mono+) dual-energy computed tomography (DECT) in patients with head and neck squamous cell carcinoma (SCC).

**Methods** DECT data of 44 patients (34 men, mean age  $55.5 \pm 16.0$  years) with histopathologically confirmed SCC were reconstructed as 40, 55, 70 keV Mono + and M<sub>0.3</sub> (30 % 80 kV) linearly blended series. Attenuation of tumour, sternocleidomastoid muscle, internal jugular vein, submandibular gland, and noise were measured. Three radiologists with >3 years of experience subjectively assessed image quality, lesion delineation, image sharpness, and noise.

**Results** The highest lesion attenuation was shown for 40 keV series ( $248.1 \pm 94.1$  HU), followed by 55 keV ( $150.2 \pm 55.5$  HU;  $P=0.001$ ). Contrast-to-noise ratio (CNR) at 40 keV ( $19.09 \pm 13.84$ ) was significantly superior to all other reconstructions (55 keV,  $10.25 \pm 9.11$ ; 70 keV,  $7.68 \pm 6.31$ ; M<sub>0.3</sub>,  $5.49 \pm 3.28$ ; all  $P < 0.005$ ). Subjective image quality was highest for 55 keV images ( $4.53$ ;  $\kappa=0.38$ ,  $P=0.003$ ), followed by 40 keV ( $4.14$ ;  $\kappa=0.43$ ,  $P < 0.001$ ) and 70 keV reconstructions ( $4.06$ ;  $\kappa=0.32$ ,  $P=0.005$ ), all superior ( $P < 0.004$ ) to linear blending M<sub>0.3</sub> ( $3.81$ ;  $\kappa=0.280$ ,  $P=0.056$ ).

**Conclusions** Mono + DECT at low keV levels significantly improves CNR and subjective image quality in patients with head and neck SCC, as tumour CNR peaks at 40 keV, and 55 keV images are preferred by observers.

## Key Points

- Mono + DECT combines increased contrast with reduced image noise, unlike linearly blended images.
- Mono + DECT imaging allows for superior CNR and subjective image quality.
- Head and neck tumour contrast-to-noise ratio peaks at 40 keV.
- 55 keV images are preferred over all other series by observers.

M. H. Albrecht (✉) · J.-E. Scholtz · J. Kraft · R. W. Bauer ·  
M. Kaup · P. Dewes · A. M. Bucher · I. Burck · T. Lehnert ·  
J. M. Kerl · T. J. Vogl · J. L. Wichmann  
Department of Diagnostic and Interventional Radiology, University  
Hospital Frankfurt, Theodor-Stern-Kai 7, 60590 Frankfurt am  
Main, Germany  
e-mail: MoritzAlbrecht@gmx.net

J. Wagenblast  
Department of Otolaryngology, Head and Neck Surgery, University  
Hospital Frankfurt, Theodor-Stern-Kai 7, 60590 Frankfurt am  
Main, Germany

J. L. Wichmann  
Department of Radiology and Radiological Science, Medical  
University of South Carolina, Charleston, SC, USA

**Keywords** Monoenergetic Plus · Dual-Energy CT ·  
Monochromatic imaging · Computed Tomography · Head and  
Neck Cancer

## Introduction

Accurate assessment and clear delineation of lesions is crucial for appropriate therapy of patients with head and neck squamous cell carcinoma (SCC) [1, 2]. For this purpose, computed tomography (CT) is the most commonly applied cross-sectional imaging modality [1, 3–5]. Recent studies comprehensively investigated the potential of dual-energy CT (DECT) technique for oncological imaging [3, 4, 6–11]. During the rapid development of DECT, various post-processing techniques have been introduced including monochromatic, also known as monoenergetic, reconstruction. The usefulness of this post-processing algorithm for reduction of metal artefacts and CT angiography is well established [12–15]. For imaging of head and neck cancer, a recent study demonstrated that virtual monoenergetic reconstruction of DECT data at 60 keV is able to improve significantly lesion enhancement, CNR, subjective overall image quality and tumour delineation [16].

Recently, the monochromatic reconstruction algorithm has been modified and an advanced monoenergetic (Mono+) technique was introduced [17, 18]. With this algorithm, a regional spatial, frequency-based recombination of the high signal at lower energies and the superior noise properties at medium energies is performed to avoid noise increase at lower calculated energies, which is a known drawback of virtual monoenergetic images at low keV levels [17]. Hereby, a frequency-split technique is used to decompose DECT data into two subimage stacks. Subsequently, a recombination of this data is performed, which is supposed to combine a superior contrast with low noise, representing the major benefits of each image set.

Initial studies investigating the Mono + technique showed an increased CNR at 40 keV [17] and a superior depiction of intrahepatic vessels [18]. However, the few existing prior studies investigating Mono + were either conducted on a phantom or investigated its general effects on CNR of iodinated contrast media. To our knowledge, the impact of this new post-processing algorithm on oncological DECT, and especially head and neck tumours, has not been evaluated so far.

Thus, the purpose of this study was to evaluate the effects of the Mono + post-processing technique on objective and subjective image quality in DECT imaging in patients with head and neck cancer and to define optimal keV settings.

## Materials and methods

### Patient selection and study design

Our local ethics committee approved this study with a waiver for written consent. Forty-four patients (34 men, mean age  $55.5 \pm 16.0$  years) with histopathologically confirmed nasopharyngeal (n=6), oropharyngeal (n=8), hypopharyngeal/laryngeal (n=15), and buccal (n=2) squamous cell carcinoma

(SCC) were retrospectively included. The other locations included tongue (n=4), floor of mouth (n=6), and nose (n=3). DECT was performed for evaluation of primary (n=20) or recurrent cancer (n=24).

### DECT protocol

The included CT examinations were performed on a dual-source CT (Somatom Definition Flash, Siemens Healthcare, Forchheim, Germany) using two x-ray tubes with different kV settings (tube A: 80 kV, tube B: 140 kV with tin filter). Furthermore, the following parameters were used: collimation,  $2 \times 64 \times 0.6$  mm; rotation time, 0.5 s; pitch 0.9; reference tube current-time product for the 140 kVp tube, 151 mAs, and for the 80 kVp tube, 302 mAs.

In all examinations, iodinated nonionic contrast agent (80 mL iopamidol, Imeron 400, Bracco, Konstanz, Germany) was administered via a peripheral vein of the antecubital fossa or dorsum of the hand with a flow of 2 mL/s followed by a 50 mL saline flush. Images were obtained 70 s after starting the injection in expiratory breath hold.

### Reconstruction of DECT data

In our study, four main image series were reconstructed using a standard DECT soft tissue kernel (D30f) and analyzed. First, a standard image stack with the linear blending technique M\_0.3 (computed by merging 30 % of the 80 kV and 70 % of the 140 kV data) was calculated to represent standard single-energy 120 kV acquisition as previously described [3, 7, 16]. Subsequently, the acquired data were post-processed using dedicated dual-energy Mono + software on a 3D workstation (syngo.via, version VA11A, Siemens Healthcare).

Mono + images were reconstructed with 40, 55, and 70 keV as previously described [17]. As recent studies investigating Mono + suggested 40 keV as the optimal spectrum with best CNR [17, 18], we did not reconstruct images at higher keV levels beyond 70 keV, since the iodine signal can be expected to be extenuated. The Mono + and the M\_0.3 image series were reconstructed as transverse images with a section width of 2.0 mm.

### Objective image analysis

A radiologist with 2 years of experience in CT imaging of head and neck reviewed all image data on a commercially available PACS workstation (Centricity 4.2, GE Healthcare, Dornstadt, Germany) using a standard reading monitor (RadiForce RX240, Eizo, Ishikawa, Japan). In all malignant lesions, ipsilateral internal jugular veins, submandibular glands, and sternocleidomastoid muscles a region of interest (ROI; size,  $12 - 36 \text{ mm}^2$ ) was placed in a representative area to measure signal attenuation in mean Hounsfield units (HU).

In case tumour necrosis was present, the ROI was placed in a peripheral vital tumour area. In general, ROIs were placed as large as possible, but with an adequate distance to surrounding anatomical structures and to avoid focal areas of heterogeneity. For measurement of image noise, a circular ROI (size,  $100 \text{ mm}^2$ ) was placed in the extracorporeal air and the standard deviation (SD) was recorded. These measurements were performed three times and resulting values were averaged to ensure data consistency.

The formula for calculating the tumour contrast-to-noise ratio (CNR) was as follows:  $\text{CNR} = (\text{average lesion enhancement/attenuation of ipsilateral sternocleidomastoideal muscle})/\text{background noise}$ , according to previous studies [3, 19]. All ROI measurements and calculated CNR were considered objective image quality parameters.

### Subjective image analysis

The image series were then separately reviewed in a random order by three radiologists with >3 years of experience in CT imaging of head and neck, respectively. The reviewers were blinded to the applied reconstruction technique but were aware that every patient had head and neck cancer with findings present on the assessed image series. In case the observers were unable to locate the lesion, the exact location of SCC was pointed out by the lead author. However, this was only performed in two cases. Images were arranged in the standard soft tissue window (level, 100; width, 400) as axial slices. Reviewers were allowed to alter the window settings and all available CT series of an axial reconstructed image stack could be assessed if required. Subjective image quality of each image series was rated using a 5-point Likert scale (1 = non-diagnostic, 2 = limited, 3 = moderate, 4 = good, 5 = excellent). Furthermore, delineation of lesion margins (ranging from 1 = no visual delineation to 5 = excellent delineation), image sharpness (ranging from 1 = distinct blurring to 5 = excellent sharpness), and image noise (ranging from 1 = extensive image noise to 5 = absence of noise) were rated.

### Statistical analysis

All statistical analyses were performed using dedicated software (MedCalc Statistical Software version 12.7.2, MedCalc Software bvba, Ostend, Belgium). Differences of all objective image quality results were analyzed by means of the Student *t* test. Subjective image quality was analyzed by averaging the reviewers' 5-point scores and using the nonparametric Friedman test with post-hoc tests. Inter-rater agreement was analyzed by means of Cohen's kappa ( $\kappa$ ) analysis. Hereby, coefficients were interpreted as follows:  $\kappa < 0.20$  = slight agreement,  $\kappa: 0.21 - 0.40$  = fair agreement,  $\kappa: 0.41 - 0.60$  = moderate agreement,  $\kappa: 0.61 - 0.80$  = substantial agreement,  $\kappa: 0.81 -$

$1.0$  = almost perfect agreement [20]. A *P*-value less than 0.05 was considered to indicate a statistically significant result.

## Results

All CT examinations were performed without occurrence of complications or severe motion or beam-hardening artefacts influencing lesion visibility. The mean volume CT dose index ( $\text{CDTI}_{\text{vol}}$ ) was  $9.88 \pm 0.52 \text{ mGy}$  and the mean dose length product (DLP) was  $272.2 \pm 24.9 \text{ mGy} \cdot \text{cm}$ .

### Objective image analysis

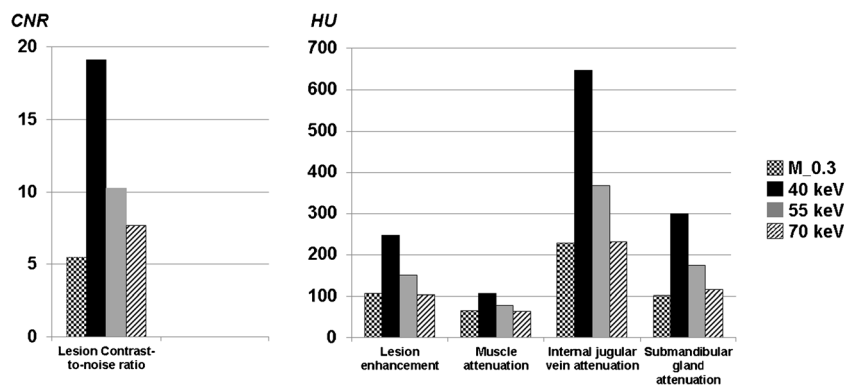
Table 1 and Fig. 1 give an overview of the results of the objective image analysis. Enhancement of SCC lesions was highest in the 40 keV series ( $248.1 \pm 94.1 \text{ HU}$ ), followed by the 55 keV reconstructions ( $150.2 \pm 55.5 \text{ HU}$ ;  $P < 0.001$ ). The linearly blended M\_0.3 series showed a significantly lower attenuation compared to the 55 keV series ( $106.0 \pm 23.5 \text{ HU}$ ;  $P < 0.001$ ), but were slightly higher compared to the 70 keV series ( $102.9 \pm 37.7 \text{ HU}$ ), however, without a significant difference ( $P = 0.643$ ).

Image noise gradually decreased from the 40 keV series ( $9.24 \pm 6.71 \text{ HU}$ ), to the 55 keV ( $8.46 \pm 7.74 \text{ HU}$ ;  $P < 0.031$ ) and 70 keV series ( $6.02 \pm 4.47 \text{ HU}$ ;  $P < 0.001$ ). There was no significant difference regarding image noise between the M\_0.3 series ( $7.45 \pm 1.77 \text{ HU}$ ) and the Mono + series ( $P < 0.405$ ).

The calculated CNR of SCC lesions were highest in the 40 keV image series ( $19.09 \pm 13.84$ ) and superior to all other Mono + reconstructions ( $P < 0.005$ ). Reconstructions at 55 keV ( $10.25 \pm 9.11$ ) showed a significantly higher lesion CNR compared to the M\_0.3 series ( $5.49 \pm 3.28$ ;  $P = 0.006$ ), but no significant difference was found between CNR of M\_0.3 and 70 keV reconstructions ( $7.68 \pm 6.31$ ;  $P = 0.165$ ).

**Table 1** Results of objective image analysis. Data are mean  $\pm$  standard deviation

Parameter	M_0.3	40 keV	55 keV	70 keV
Lesion enhancement (HU)	106.0 $\pm 23.5$	248.1 $\pm 94.1$	150.2 $\pm 55.5$	102.9 $\pm 37.7$
Muscle attenuation (HU)	65.7 $\pm 8.5$	106.0 $\pm 41.3$	78.0 $\pm 24.2$	63.1 $\pm 14.4$
Noise (HU)	7.45 $\pm 1.77$	9.24 $\pm 6.71$	8.46 $\pm 7.74$	6.02 $\pm 4.47$
Lesion contrast-to-noise ratio (CNR)	5.49 $\pm 3.28$	19.09 $\pm 13.84$	10.25 $\pm 9.11$	7.68 $\pm 6.31$
Internal jugular vein attenuation (HU)	228.2 $\pm 71.5$	647.3 $\pm 145.7$	367.7 $\pm 77.8$	231.3 $\pm 47.9$
Submandibular gland attenuation (HU)	102.2 $\pm 27.8$	299.6 $\pm 92.6$	174.9 $\pm 50.5$	115.9 $\pm 31.2$



**Fig. 1** Results from the objective image analysis. The Mono + series showed a superior attenuation regarding all parameters. This was most distinct for the 40 keV series, for which contrast-to-noise ratio and internal jugular vein attenuation were more than twofold compared to the M\_0.3 and 70 keV reconstructed images ( $P < 0.001$ ). Furthermore, 40 keV

images showed an 87 % higher CNR and 76 % higher attenuation of the internal jugular vein compared to the 55 keV series ( $P < 0.001$ ). No significant differences were found between the M\_0.3 and 70 keV series except for submandibular gland attenuation ( $P < 0.001$ ).

Further details from objective image analysis of SCC lesions are summarized in Table 1.

Enhancement of the sternocleidomastoid muscle peaked in the 40 keV series ( $106.0 \pm 41.3$  HU). All differences between the other image series were significant ( $P < 0.001$ ) except between the M\_0.3 and the 70 keV series ( $P = 0.256$ ).

Signal attenuation in the internal jugular vein gradually decreased from the 40 keV series ( $647.3 \pm 145.7$  HU), the 55 keV ( $367.7$  HU  $\pm 77.8$ ;  $P < 0.001$ ), and the 70 keV ( $231.3 \pm 47.9$  HU;  $P = 0.009$ ) series. Venous attenuation was  $228.2 \pm 71.5$  HU for the M\_0.3 series with significant differences compared to the 40 and 55 keV Mono+reconstructions ( $P < 0.001$ ), but not compared to the 70 keV series ( $P = 0.817$ ). Similarly, attenuation of the submandibular gland peaked in the 40 keV series ( $299.6 \pm 92.6$  HU) followed by 55 keV ( $174.9 \pm 50.5$  HU;  $P < 0.001$ ) and the M\_0.3 series ( $102.2 \pm 27.5$  HU;  $P < 0.001$ ).

### Subjective image analysis

The median values with related  $P$ -values and Kappa coefficients of the reviewers' image quality scores are summarized in Table 2. Figures 2, 3 and 4 demonstrate the different image

impression of head and neck DECT images at M\_0.3 and Mono + reconstructions with various keV levels in our study.

The mean rating of overall subjective image quality was highest for the 55 keV+ reconstructions with slight inter-rater agreement ( $4.53$ ;  $\kappa = 0.38$ ,  $P = 0.003$ ), followed by 40 keV ( $4.14$ ;  $\kappa = 0.43$ ,  $P = < 0.001$ ) and 70 keV reconstructions ( $4.06$ ;  $\kappa = 0.32$ ,  $P = 0.005$ ). The differences between 55 keV to 40 and 70 keV, respectively, were significant ( $P < 0.001$ ), but not for comparing 40 and 70 keV ( $P = 0.465$ ). All Mono+ series were rated superior ( $P < 0.004$ ) to the linear blending setting M\_0.3 ( $3.81$ ;  $\kappa = 0.280$ ,  $P = 0.056$ ).

Subjective evaluation of tumour delineation also peaked in the 55 keV reconstructions ( $4.68$ ;  $\kappa = 0.31$ ,  $P = 0.005$ ) and was higher than for the M\_0.3 series ( $3.70$ ;  $\kappa = 0.238$ ,  $P = 0.036$ ) and the other Mono + series (all  $P < 0.028$ ). There was no significant difference regarding tumour delineation between the M\_0.3 and 70 keV series ( $P = 0.061$ ).

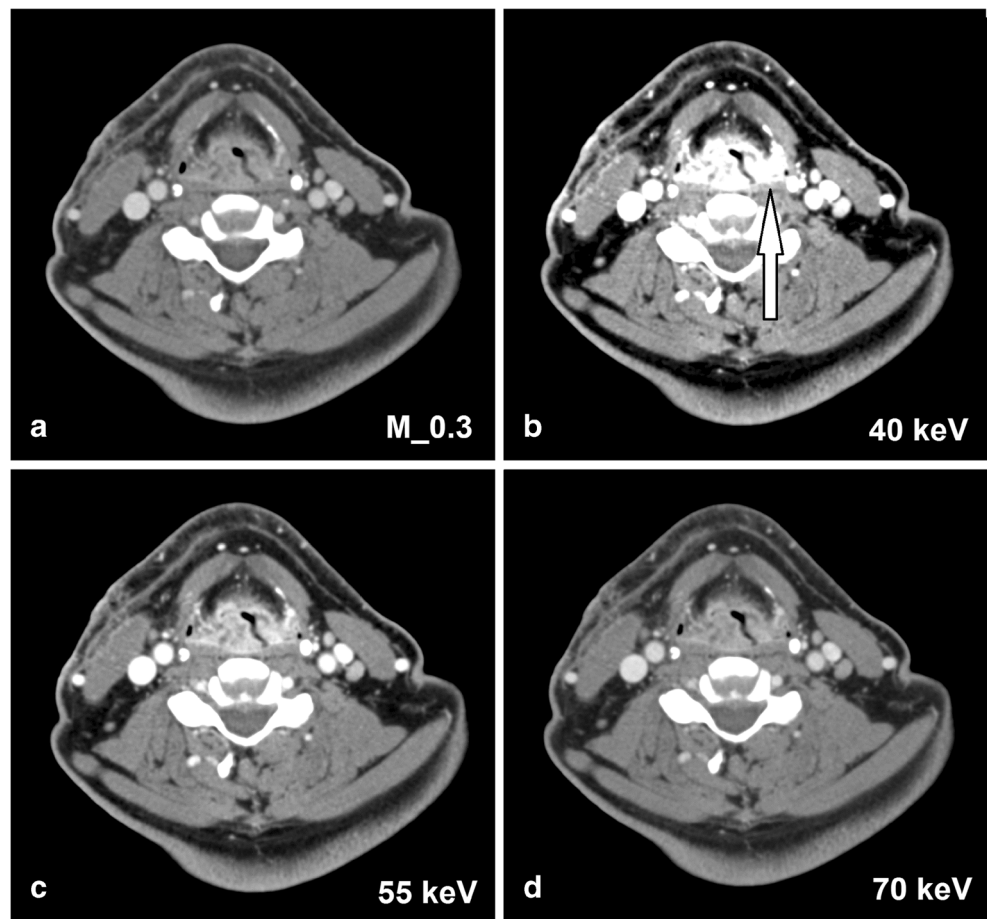
The 70 keV reconstructions received the best rating regarding image sharpness ( $4.40$ ;  $\kappa = 0.26$ ,  $P = 0.003$ ), followed by 55 keV ( $4.29$ ;  $\kappa = 0.31$ ,  $P = 0.003$ ), 40 keV ( $4.12$ ;  $\kappa = 0.25$ ;  $P = 0.01$ ) and M\_0.3 ( $3.70$ ;  $\kappa = 0.419$ ,  $P = 0.001$ ). All differences indicated a statistical significance ( $P < 0.008$ ) except the comparison of 55 and 70 keV ( $P = 0.256$ ).

**Table 2** Results of subjective image analysis

Image series	Overall image quality	Delineation of lesion	Image sharpness	Absence of image noise
M_0.3	<b>3.81</b> [0.280; 0.056]	<b>3.70</b> [0.238; 0.036]	<b>3.70</b> [0.419; <0.001]	<b>3.96</b> [0.419; <0.001]
40 keV	<b>4.14</b> [0.43; <0.001]	<b>4.49</b> [0.30; <0.001]	<b>4.12</b> [0.25; 0.010]	<b>4.05</b> [0.62; <0.001]
55 keV	<b>4.53</b> [0.38; 0.003]	<b>4.68</b> [0.31; 0.005]	<b>4.29</b> [0.31; 0.003]	<b>4.39</b> [0.61; <0.001]
70 keV	<b>4.06</b> [0.32; 0.005]	<b>3.81</b> [0.27; <0.001]	<b>4.40</b> [0.26; 0.003]	<b>4.70</b> [0.58; <0.001]

Bold values represent mean data based on the ratings from all three observers. Kappa values  $\kappa$  with related  $P$ -values are displayed in brackets [ $\kappa =$ ;  $P =$ ]

**Fig. 2** Axial CT images of a 62 year-old male patient with findings of a laryngeal supraglottic SCC with invasion of the epiglottis and sinus piriformis. A substantially increased lesion attenuation is shown in the virtual monoenergetic 40 keV images (b) with an improved lesion delineation (arrow). However, 55 keV images (c) received the best scores regarding subjective image quality analysis due to a more homogeneous attenuation without overexposure. Reconstructions at 70 keV (d) showed the least image noise, but simultaneously lesion and vessel attenuation were lower than at 40 keV and 55 keV. All Mono+ series were subjectively rated superior compared to the M\_0.3 images (a) regarding all assessed criteria. (Window settings: level, 100; width, 400)



The 70 keV reconstructions received the best subjective rating regarding absence of image noise with substantial agreement (4.70;  $\kappa=0.58$ ,  $P<0.001$ ), linearly followed by 55 keV (4.39;  $\kappa=0.61$ ;  $P<0.001$ ) and 40 keV (4.05; 0.62;  $P<0.001$ ) reconstructions and superior to the M\_0.3 series (3.96;  $\kappa=0.419$ ;  $P<0.001$ ). All differences were significant ( $P<0.003$ ) except when comparing M\_0.3 and 40 keV ( $P<0.161$ ).

## Discussion

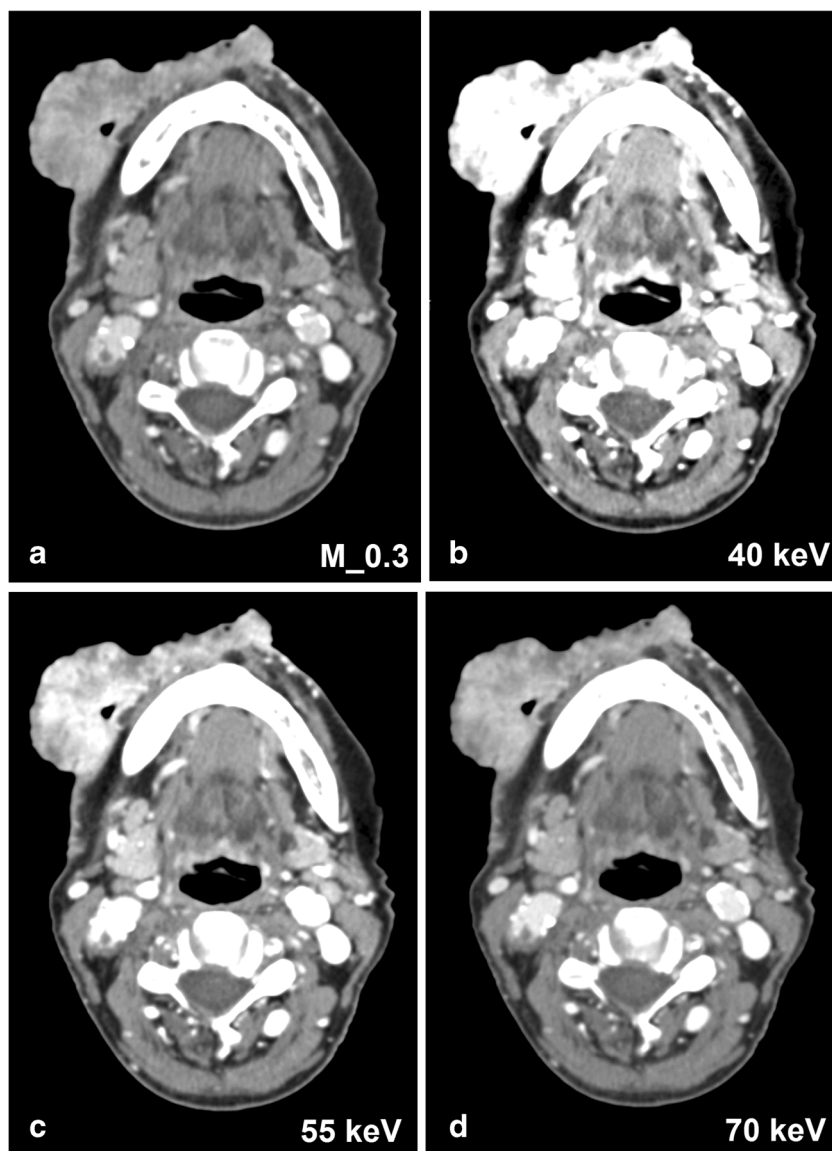
In this study we aimed to evaluate the impact of the Mono + reconstruction technique on subjective and objective image quality compared to linearly blended DECT images in patients with head and neck cancer and to define optimal keV settings. Calculation of virtual monoenergetic images from DECT data allows for reconstruction at different keV levels. Traditionally, at lower energy levels, a superior lesion contrast to surrounding tissue can be achieved through an increased iodine attenuation, but simultaneously a higher image noise is observed. Thus, images at low keV levels may not necessarily result in an improved CNR as previously described [17, 21]. Hereby, the novel Mono + algorithm has shown promising results in recent studies [17, 18] to overcome this limitation and to

combine the higher contrast at lower keV parameters with a low image noise at higher keV levels and, therefore, ultimately allow for a superior CNR compared to standard single-energy CT and linearly blended images.

In the objective image analysis, we found that attenuation of SCC lesions at 40 keV was significantly superior to the other Mono + and the linearly blended M\_0.3 series ( $P<0.001$ ). Although the image noise also peaked in this series, the substantially increased attenuation ultimately resulted in the highest CNR in our study with a mean value of 19.09. Furthermore, muscle attenuation of the sternocleidomastoid muscle, internal jugular vein, and submandibular gland were also significantly superior in the 40 keV series ( $P<0.009$ ). These findings are in accordance to a previous study, which demonstrated that the Mono + technique provided increasing iodine CNR with decreasing keV levels, with an optimum CNR obtained at 40 keV regarding artificial lesions of four circular phantoms and an anthropomorphic abdominal phantom [17].

However, the subjective image analysis in our study revealed 55 keV series as the image reconstruction of choice regarding subjective image quality and delineation of lesions. This indicates that the strongest attenuation of SCC lesions at 40 keV does not automatically result in a superior subjective image quality for imaging of head and neck cancer. Image

**Fig. 3** Transversal images of a 67 year-old patient with a SCC arising from the soft tissue of the right mandible. The 40 keV DECT image series (b) reveals a distinct iodine attenuation of the tumour compared to the other series. Despite the lower CNR, images at 55 keV (c) show with sufficient lesion delineation the most details regarding the inhomogeneous tissue and contrast enhancement. Linearly blended M<sub>0.3</sub> images (a) and 70 keV reconstructions (d) show similar lesion attenuation, lower compared to reconstructions at 40 keV and 55 keV. (Window settings: level, 100; width, 400)

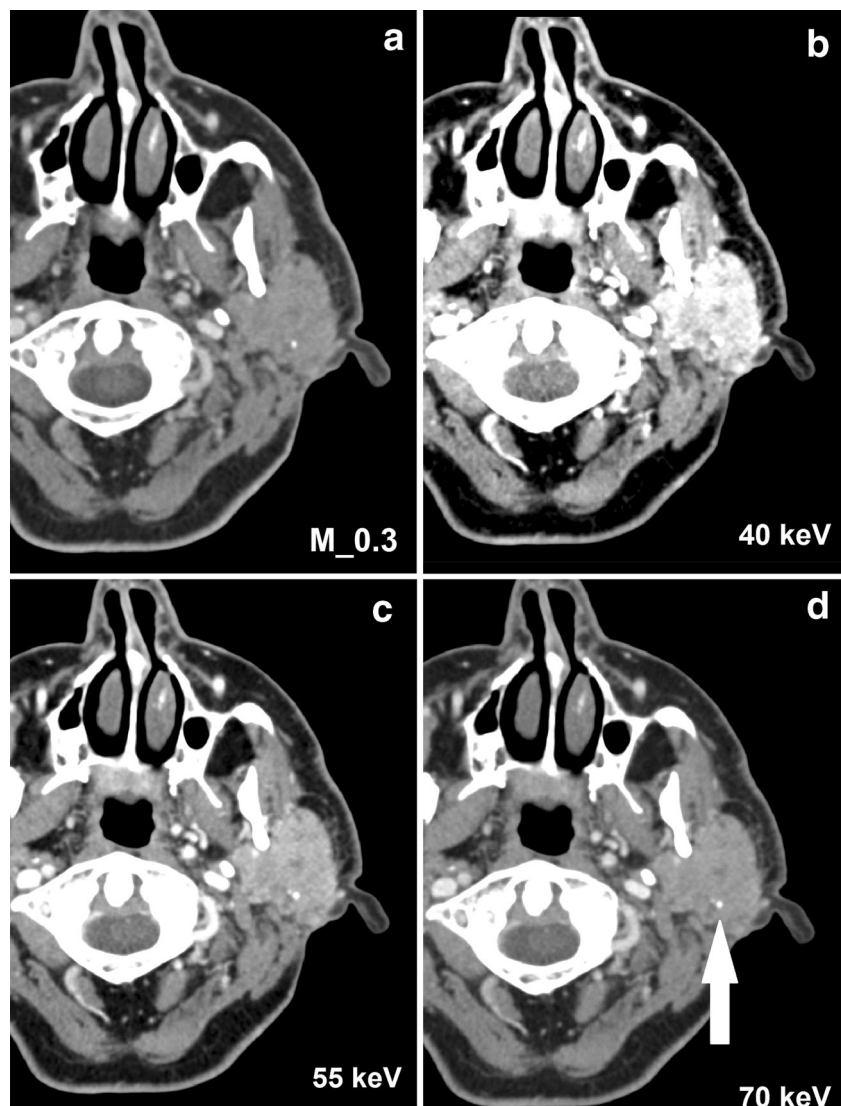


noise seems to have a substantial impact on subjective image quality. Hereby, prior studies have also indicated that subjective evaluation by clinical radiologists might not necessarily coincide with objective measurements [3, 22]. Based on our results, we would recommend using 55 keV in clinical practice rather than linearly images or other monoenergetic energy levels in head and neck cancer imaging. Reconstruction at 55 keV appears to be a reasonable compromise regarding lesion CNR and image noise. However, the optimal Mono + keV settings need to be re-evaluated in future studies, as well as the impact of Mono + DECT on diagnostic accuracy.

As opposed to our results, in a recent study, Schabel et al. assessed the hepatic veins in poor contrast conditions using Mono + calculated DECT images and found in a subjective analysis that Mono + at 40 keV received the best ratings for depiction and assessment for intrahepatic vessels [18]. However, the comparability of this study with ours is somewhat

limited, because signal attenuation and image noise can be expected to differ between abdominal and head and neck imaging due to an enlarged body circumference and more surrounding soft tissue. Although intravascular attenuation also peaked in the 40 keV series in our study, this may have influenced subjective image quality more than in our study, as Schabel et al. focused explicitly on intrahepatic vessels with poor contrast conditions. Recently, Grant et al. investigated the Mono + algorithm for evaluation of objective image quality of iodinated contrast media in an anthropomorphic phantom and also reported that reconstructions at 40 keV provided the best CNR [17]. Nevertheless, as experience with the Mono + technique currently remains scarce, we hypothesize that assessing the most appropriate keV level of DECT data using the Mono + algorithm might vary over a certain range for different anatomical regions, which should be investigated in future studies, especially for oncological imaging.

**Fig. 4** Transversal sections showing a 67 year-old patient's SCC lesion located in the left parotid gland. A synchronous ipsilateral lymph node metastasis is also present. Whereas a calcification (*arrow*) within the tumour is distinctly delineated from the surrounding malignant tissue in the 55 keV series (c), demarcation of the calcification in the 40 keV images (b) is complicated by an overexposing iodine attenuation at 40 keV. Linearly blended M<sub>0.3</sub> (a) and 70 keV (d) images show decreased tumour attenuation. (Window settings: level, 100; width, 400)



Furthermore, due to the increased CNR at lower keV levels, it was presumed in recent studies that the Mono + technique may allow for a comparable image quality on contrast-enhanced CT with a reduced amount of administered contrast media, from which patients with reduced kidney function might benefit [18, 23]. Although this was not the topic of our study, we concur with this assumption as the substantially increased attenuation and CNR at 40 keV found in our study might indeed allow for a contrast media reduction especially during carotid-cerebrovascular CT angiography which should be assessed in future studies.

In our study, all Mono + series were subjectively rated superior concerning all assessed criteria in comparison to the M<sub>0.3</sub> series except for image noise between the M<sub>0.3</sub> and 40 keV series. This applied especially to the 40 keV series, whereas Wichmann et al. found that traditional monoenergetic reconstructions of DECT data at 40 keV were inferior to M<sub>0.3</sub> regarding overall image quality, delineation of lesions, image

sharpness and noise for imaging of head and neck cancer due to a far more severe noise signal [16]. Thus, with the Mono + technique, reconstruction levels of 40 and 55 keV may be optimal for most imaging indications, while most studies reported an optimal level of 60 – 70 keV with the traditional monoenergetic reconstruction algorithm [14, 16, 24].

Our study has several limitations that should be addressed. First, we only compared Mono + calculated images with M<sub>0.3</sub> series as this is the standard linear blending setting on the used DECT system. When interpreting our results, it has to be taken into account that prior studies indicated that reconstruction using the M<sub>0.5</sub> or M<sub>0.6</sub> parameter might be superior to M<sub>0.3</sub> [3, 25]. However, the increase in signal attenuation and CNR with the Mono + image series was so distinct compared to M<sub>0.3</sub>, that we expect significant differences for these parameters even in comparison with reconstruction using M<sub>0.5</sub> or M<sub>0.6</sub> parameters. Second, reviewers were aware that only patients with head and neck

cancer were included in this study. This might have influenced the ratings especially regarding tumour delineation and lesion enhancement due to a greater diagnostic confidence [3]. In this context, we also did not specifically investigate the impact of the Mono + technique on diagnostic accuracy, although we assume that an improved CNR may at least result in a comparable diagnostic accuracy. Furthermore, a recent study even demonstrated a comparable sensitivity and specificity for the detection of head and neck SCC for evaluation at 80 kV, which also resulted in a superior CNR and subjective tumor delineation compared to standard linearly blended images [26]. Third, we also did not directly compare traditional monoenergetic to Mono + images. When correlating recent studies investigating monoenergetic DECT imaging to ours, it has to be taken into account that monoenergetic and Mono + images cannot be unrestrictedly compared at identical keV levels, as the postprocessing algorithms fundamentally differ. Nevertheless, as the Mono + algorithm has been introduced as the new standard algorithm for monoenergetic reconstructions for the workstation used in our study, we expect additional studies investigating differences between Mono + and the traditional monoenergetic algorithm in the future.

## Conclusion

Image reconstruction at low keV levels using the novel advanced Mono + algorithm objectively enables an increased lesion attenuation at simultaneously low image noise, especially at 40 keV, resulting in a superior CNR compared to standard linear blending. However, images at 55 keV were rated superior regarding subjective image analysis which might therefore be the preferential setting in routine clinical practice.

**Acknowledgements** The scientific guarantor of this publication is Dr Julian L. Wichmann. The authors of this manuscript declare relationships with the following companies: Ralf W. Bauer and J. Matthias Kerl are on the speakers' bureau of Siemens Healthcare, Computed Tomography division. The other authors of this manuscript declare no relationships with any companies, whose products or services may be related to the subject matter of the article. The authors state that this work has not received any funding. One of the authors has significant statistical expertise. Institutional review board approval was obtained.

Written informed consent was waived by the institutional review board. No study subjects or cohorts have been previously reported. Methodology: retrospective, case-control study, performed at one institution.

## References

- Sadick M, Schoenberg SO, Hoermann K, Sadick H (2012) Current oncologic concepts and emerging techniques for imaging of head and neck squamous cell cancer. *GMS Curr Top Otorhinolaryngol Head Neck Surg* 11:Doc08
- Hermans R (2006) Staging of laryngeal and hypopharyngeal cancer: value of imaging studies. *Eur Radiol* 16:2386–2400
- Tawfik AM, Kerl JM, Bauer RW et al (2012) Dual-energy CT of head and neck cancer: average weighting of low- and high-voltage acquisitions to improve lesion delineation and image quality-initial clinical experience. *Invest Radiol* 47:306–311
- Toepker M, Czerny C, Ringl H et al (2014) Can dual-energy CT improve the assessment of tumor margins in oral cancer? *Oral Oncol* 50:221–227
- Geets X, Daisne J-F, Arcangeli S et al (2005) Inter-observer variability in the delineation of pharyngo-laryngeal tumor, parotid glands and cervical spinal cord: comparison between CT-scan and MRI. *Radiother Oncol* 77:25–31
- Vogl TJ, Schulz B, Bauer RW et al (2012) Dual-energy CT applications in head and neck imaging. *AJR Am J Roentgenol* 199:S34–S39
- Tawfik AM, Kerl JM, Razek AA et al (2011) Image quality and radiation dose of dual-energy CT of the head and neck compared with a standard 120-kVp acquisition. *AJNR Am J Neuroradiol* 32:1994–1999
- Paul J, Vogl TJ, Mbalisike EC (2014) Oncological applications of dual-energy computed tomography imaging. *J Comput Assist Tomogr* 38:834–842
- Paul J, Mbalisike EC, Nour-Eldin N-EA, Vogl TJ (2013) Dual-source 128-slice MDCT neck: radiation dose and image quality estimation of three different protocols. *Eur J Radiol* 82:787–796
- De Cecco CN, Damell A, Rengo M et al (2012) Dual-energy CT: oncologic applications. *AJR Am J Roentgenol* 199:S98–S105
- Simons D, Kachelriess M, Schlemmer H-P (2014) Recent developments of dual-energy CT in oncology. *Eur Radiol* 24:930–939
- Bamberg F, Dierks A, Nikolaou K et al (2011) Metal artifact reduction by dual energy computed tomography using monoenergetic extrapolation. *Eur Radiol* 21:1424–1429
- Stolzmann P, Winklhofer S, Schwendener N et al (2013) Monoenergetic computed tomography reconstructions reduce beam hardening artifacts from dental restorations. *Forensic Sci Med Pathol* 9:327–332
- Schneider D, Apfaltrer P, Sudarski S et al (2014) Optimization of kiloelectron volt settings in cerebral and cervical dual-energy CT angiography determined with virtual monoenergetic imaging. *Acad Radiol* 21:431–436
- Apfaltrer P, Sudarski S, Schneider D et al (2014) Value of monoenergetic low-kV dual energy CT datasets for improved image quality of CT pulmonary angiography. *Eur J Radiol* 83:322–328
- Wichmann JL, Nöske E-M, Kraft J et al (2014) Virtual monoenergetic dual-energy computed tomography: optimization of kiloelectron volt settings in head and neck cancer. *Invest Radiol* 49:735–741
- Grant KL, Flohr TG, Krauss B et al (2014) Assessment of an advanced image-based technique to calculate virtual monoenergetic computed tomographic images from a dual-energy examination to improve contrast-to-noise ratio in examinations using iodinated contrast media. *Invest Radiol* 49:586–592
- Schabel C, Bongers M, Sedlmair M et al (2014) Assessment of the hepatic veins in poor contrast conditions using dual energy CT: evaluation of a novel monoenergetic extrapolation software algorithm. *Röfo* 186:591–597
- Szucs-Farkas Z, Kurmann L, Strautz T et al (2008) Patient exposure and image quality of low-dose pulmonary computed tomography angiography: comparison of 100- and 80-kVp protocols. *Invest Radiol* 43:871–876
- Cohen J (1960) A coefficient of agreement for nominal scales. *Educ Psychol Meas* 20:37–46
- Delesalle M-A, Pontana F, Duhamel A et al (2013) Spectral optimization of chest CT angiography with reduced iodine load: experience in 80 patients evaluated with dual-source, dual-energy CT. *Radiology* 267:256–266
- Marin D, Nelson RC, Samei E et al (2009) Hypervascular liver tumors: low tube voltage, high tube current multidetector CT during

- late hepatic arterial phase for detection—initial clinical experience. *Radiology* 251:771–779
23. Davenport MS, Khalatbari S, Cohan RH et al (2013) Contrast material-induced nephrotoxicity and intravenous low-osmolality iodinated contrast material: risk stratification by using estimated glomerular filtration rate. *Radiology* 268:719–728
  24. Sudarski S, Apfaltrer P, Nance JW et al (2014) Objective and subjective image quality of liver parenchyma and hepatic metastases with virtual monoenergetic dual-source dual-energy CT reconstructions: an analysis in patients with gastrointestinal stromal tumor. *Acad Radiol* 21:514–522
  25. Behrendt FF, Schmidt B, Plumhans C et al (2009) Image fusion in dual energy computed tomography: effect on contrast enhancement, signal-to-noise ratio and image quality in computed tomography angiography. *Invest Radiol* 44:1–6
  26. Wichmann JL, Kraft J, Nöske E-M, et al (2014) Low-tube-voltage 80-kVp neck CT: evaluation of diagnostic accuracy and interobserver agreement. *Am J Neuroradiol*